2079 IEPC-93-221

Development and Testing of a 100 kW Radiation Cooled Thermal Hydrogen Arcjet Thruster

Thomas M. Gölz, Monika Auweter-Kurtz, and Helmut L. Kurtz
Institut für Raumfahrtsysteme
Universität Stuttgart
Pfaffenwaldring 31, D-70550 Stuttgart
Federal Republic of Germany

Abstract

Based on the water cooled High Power Arcjet HIPARC designed for the 100 kW power level and operated with hydrogen as propellant, a radiation cooled thermal arcjet thruster called HIPARC-R has been developed and constructed.

Significant improvements in performance could be achieved by changing the cooling concept. A maximum specific impulse of 2050 s could be obtained at the 100 kW power level at a mass flow rate of 150 mg/s. This equals a specific input power value of 670 MJ/kg. Total efficiency was at about 28 %. Experimental data is given for operation at four different mass flow rates.

Introduction

The development of high power thermal arcjet thrusters has been an essential research topic at Stuttgart University's Space Systems Institute (Institut für Raumfahrtsysteme, IRS). As a first step, water cooled thrusters have been developed and tested. Beginning with a 50 kW thruster device this development has led to the design and construction of a 100 kW arcjet called HIPARC. It has undergone a variety of tests which have yielded a geometry suitable for high specific impulse operation as well as high power operation.

It showed that high specific impulse values can be achieved even with water cooled devices, if only the specific input power can be increased over a certain level. It was possible to reach a maximum specific impulse of 1500 s at a maximum specific input power value of 500 MJ/kg at an efficiency of about 20 %.

In order to increase the limit of specific input power and the thrust efficiency, a radiation cooled 100 kW thruster was designed and built at IRS.

Experimental Setup

Thruster

HIPARC-R is a constrictor type thermal arcjet with a conical nozzle at a half angle of 20°. The nozzle throat diameter is 4 mm, the constrictor length to diameter ratio is 1, the area ratio is 1:225. The converging part of the nozzle offers a 50° opening half angle. These parameters have been tested before with the water cooled device ([1, 2], Mod. 2 and Mod. 3 thruster).

Although with the water cooled HIPARC the best specific impulse value could be obtained with a nozzle throat diameter of 6 mm, a 4 mm nozzle throat diameter was chosen for the radiation cooled version in order to get higher arc chamber pressures and hence better efficiencies.

The cathode of 10 mm in diameter is mounted on the gas supply tube in the thruster's centerline. This diameter proved to be the best suited for this power level with the water cooled device [1]. The cathode tip is conical with a half angle of 30°.

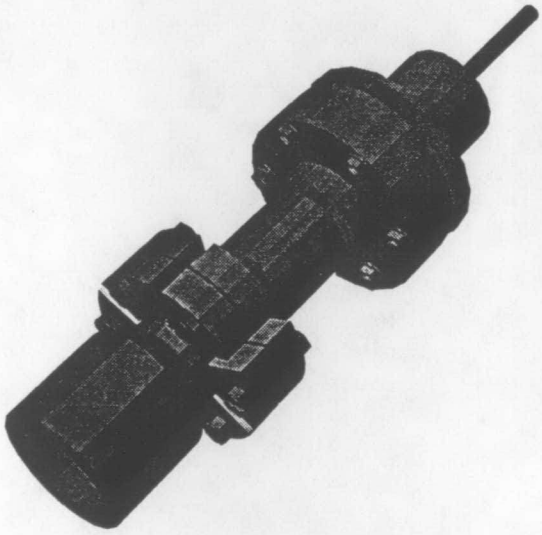

Fig. 1: Three dimensional view of HIPARC-R

The most striking feature of HIPARC-R is the big nozzle corpus, which is fixed to the thruster housing by six pairs of TZM brackets (Fig. 1). These brackets ensure that the necessary force is exerted on the graphite sealing between nozzle body and thruster housing. This solution was selected because of cost and mass saving reasons.

The nozzle dimensioning of HIPARC-R was based on thermal efficiency measurement data (obtained

with HIPARC [1, 2], data obtained with the 10 kW class thermal arcjet thrusters TT1 [3] and MARC [4]), and data published by Sankovic and Curran [5]. A total of about 10 % of the input power was expected to be radiated off the thruster at an emissivity of 0.4. A maximum nozzle temperature of 2300 K led to an outer nozzle diameter of 70 mm at a length of 72 mm.

The thruster sealing is done by graphite foil rings of 0.35 mm thickness. The sealing pressure force is supplied by the TZM brackets between nozzle and housing, by steel disks on the back side and by a spring made of *Haynes alloy 230®* inside the thruster.

The propellant gas is fed through a stainless steel pipe at the thruster center. It is used as current supply and as cathode fixation. The gas is hereby used as the current supply cooling medium. It exits the pipe near the spring and is led to a channel between the thruster housing and main isolator, where it is heated regeneratively. It is injected into the arc chamber through four bore holes (of 0.75 mm in diameter each) directing axially to the cathode tip. A swirl is not induced.

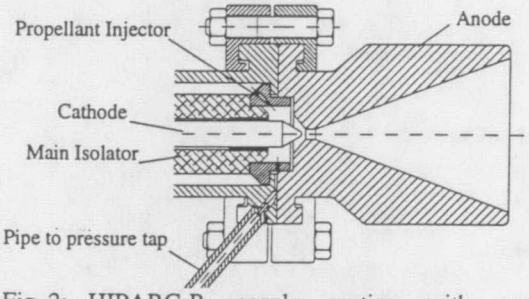

Fig. 2: HIPARC-R nozzle section with arc chamber pressure measurement access.

HIPARC-R gives the possibility to measure the arc chamber pressure during thruster operation. A TZM pipe is screwed to the thruster housing, leading to a pressure tap (Fig. 2). The pipe is water cooled by a cooling sleeve at a distance of 30 cm off the thruster. It was intended to keep the temperature gradient and thus the heat conduction along the pipe as small as possible in order not to disturb the temperature distribution in the thruster.

Cathode and anode are electrically isolated by parts made of boron nitride and a glass ceramics material (*Macor®*) , respectively.

The cathode gap can be adjusted by a mechanism that allows adjusting before sealing the cathode pipe feed through. This adjustment device is covered by a steatite cap in order to prevent arc-overs to the thruster parts on anode potential.

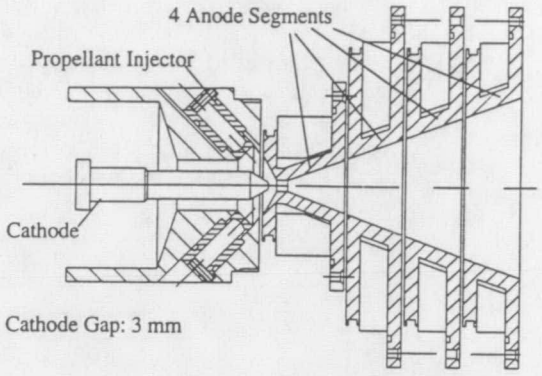

Fig. 3: Water Cooled HIPARC; Cathode/Nozzle Section.

Differences between HIPARC and HIPARC-R

The radiation cooled thruster HIPARC-R differs in some points from its water cooled predecessor HIPARC. While HIPARC was tested with three different nozzle throat diameters (6 mm, 4 mm, and 2.5 mm), HIPARC-R has been tested with the 4 mm nozzle throat diameter only. The cathode diameter is 10 mm in HIPARC-R, where cathode diameters of 5 mm , 10 mm and 14 mm had been realized in the water cooled device. The nozzle exit diameter is 64.3 mm in the water cooled thruster compared to 60 mm in the radiation cooled device. This yields a nozzle exit to throat area ratio of 1:225 with the radiation cooled thruster compared to 1:258 with the water cooled arcjet at a nozzle throat diameter of 4 mm. Due to the segmented anode the nozzle wall is interrupted by slits at HIPARC (Fig. 3). These slits are not present at HIPARC-R (Fig. 4).

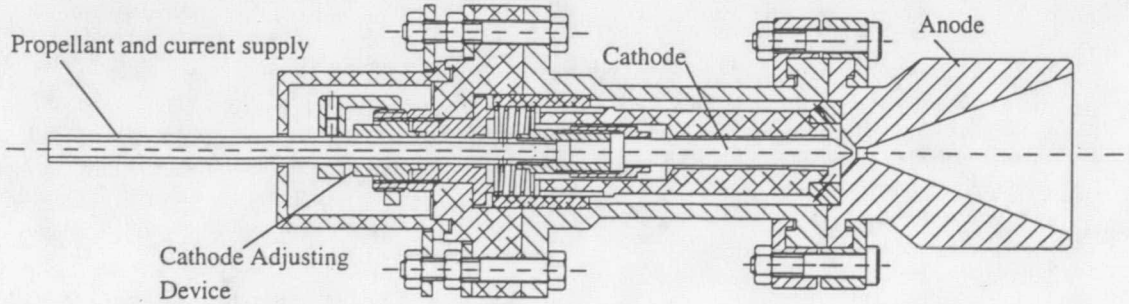

Fig. 4: Schematic drawing of HIPARC-R thruster.

Thrust Balance

The HIPARC-R thruster is mounted on the same thrust balance that was used for its watercooled predecessor HIPARC, which is an improved version of the IRS standard type (Fig. 5, [6]). The movable part of the balance carrying the thruster is suspended on three swing arms. Each swing arm is supported by two knife edge bearings.

The thrust force is transmitted as a tension force by a thin wire over a reversing sheave to a water cooled measuring box containing the force transducer. In order to allow the calibration of the balance under vacuum conditions, a remotely operated weight lever has been installed. This lever places a weight on a scale which creates a defined force on the platform.

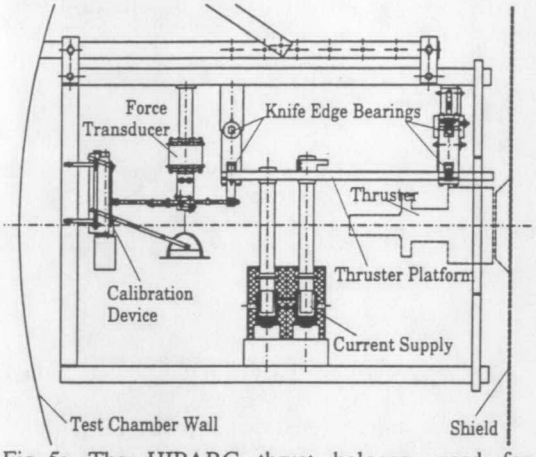

Fig. 5: The HIPARC thrust balance, used for HIPARC-R as well.

The electric power is fed to the thruster via two copper rods submerged into mercury filled tubes. To avoid evaporation of the mercury, its surface is sealed by silicon oil.

The cooling water for the thruster/thrust balance interface and for the thrust balance structure will be fed to the platform by semicircular hoses allowing minimum stiffness. Effects of stiffness and friction are calibrated for each measuring sequence before ignition and checked after engine shut down under vacuum conditions.

Test Facilities

The HIPARC-R thruster and the thrust balance are integrated in a stainless steel tank of 4.5 m length and 2 m in diameter. This vacuum chamber is double-walled in order to provide water cooling of the tank during thruster operation. The vacuum system, the high current supply, and the data acquisition system have been described in formerly published reports [3, 6].

Three mass flow controllers calibrated for hydrogen have been integrated into the IRS gas supply system, enabling a wide range of propellant gas flows to be tested. The mass flow controller readout is checked by weight-balancing of the gas bottles with an accuracy of ±1 g.

Performance Data

General Remarks

The data presented here represent results of first experiments performed with the new 100 kW thruster. The thruster limits have not been reached yet, because in this early phase of testing the risk of a catastrophic failure had to be kept as small as possible.

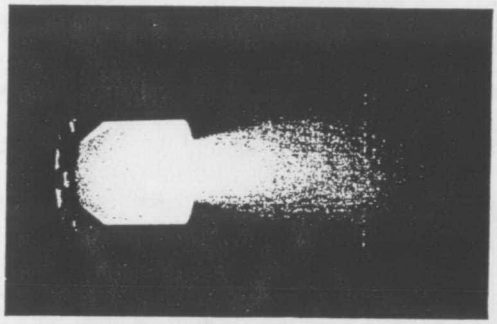

Fig. 6: HIPARC-R in operation

The measurement of the arc chamber pressure was regarded a critical step. Especially at high power levels it was not clear whether the seals and fittings could withstand the high temperatures.

Thermal Behaviour

The thruster begins heating up immediately after ignition. The temperature of a spot on the outer nozzle surface is monitored with a linear pyrometer (Type IKE LP2/80-20, [7]). The spot is located 5 mm behind the nozzle's front edge. This temperature is taken as an indicator for the temperature distribution in the thruster.

A temperature distribution measurement of the nozzle/bracket region was taken by means of a CID-camera [8], equipped with an interference filter with a bandpass of 10 nm at 797 nm in order to eliminate any line radiation that might be emitted by the various species in the plasma, so that only the portion of black body radiation is taken into account. A neutral density filter (ND4) is used in addition to adjust the sensibility of the camera to the expected intensity of radiation. The camera is calibrated by means of a black body radiator [7].

At each current setting, the temperature field tends to steady state conditions. (Fig. 7). When the current is set to a higher value, the input power is set to a higher value as well and thus the temperature rises. Consequently, the arc chamber pressure rises.

Here two opposite effects are to be reported: Firstly, the arc voltage tends to rise because of the higher pressure in the arc chamber (decreases electric conductivity), which leads to a higher input power

(the current supply system is current regulated) and again to higher temperature values. Secondly, the voltage tends to fall because of the higher gas temperature (increases electric conductivity).

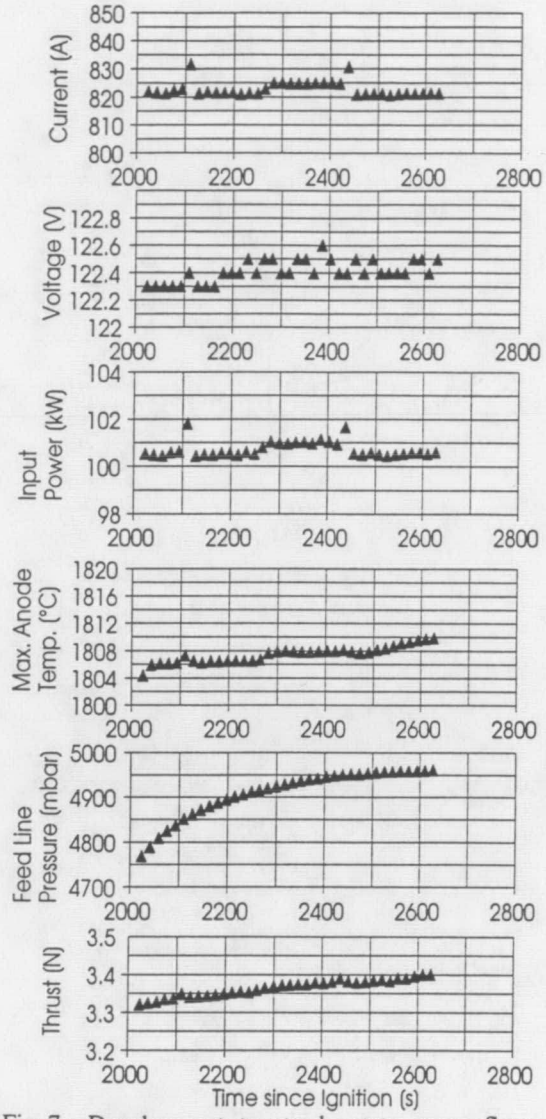

Fig. 7: Development to steady state; mass flow rate is 200 mg/s.

After the shut off the thruster cools down as is depicted in Fig. 8. Thrust and arc chamber pressure values are higher than obtained with a cold thruster. The leftmost points represent the values with the thruster still in operation.

During operation at high specific input power the cooling effect of the propellant mass flow is insufficient, so that the propellant feed tube becomes glowing.

Large temperature gradients can be observed between the nozzle body, the fixation brackets and the thruster housing. The housing temperature cannot be determined by means of this apparatus, so the temperature is lower than 1000°C.

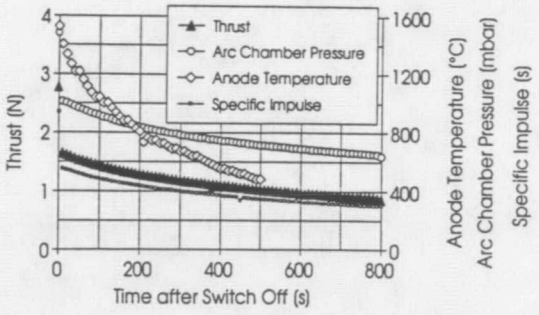

Fig. 8: Thruster cooling down characteristics

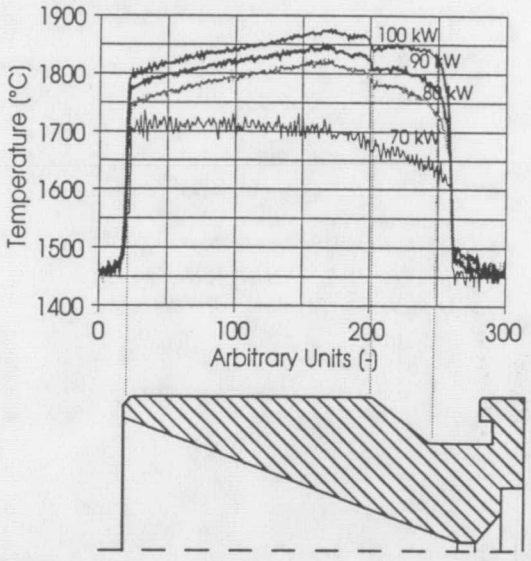

Fig. 9: Temperature distribution on the nozzle centerline.

The camera measurement of the temperature field indicates that the region of maximum temperature is located more towards the rear section of the cylindrical nozzle part. Fig. 9 shows the temperatures taken on the centerline of the nozzle corpus including the conical part. The curves represent data taken at different power levels. It can be seen that the maximum temperature rises quickly between 70 kW and 80 kW, with the region of maximum temperature moving to the back part of the cylindrical section. The temperatures in the cylindrical part then grow more slowly, whereas the cylindrical part surrounding the throat region is still heating up significantly with power.

This temperature development with input power corresponds with the arc attachment zone indicated by the current distribution measurement with the water cooled HIPARC (Fig. 10, [1]). At low power levels the main part of the current could be detected closer to the nozzle end (Seg. 4), whereas the regions close to the constrictor (Seg. 1) increase their current portion with increasing power.

Fig. 11 gives the temperature development with input power. A function of the form $T = a \cdot \sqrt[4]{P_{el}}$ was fitted to the pyrometer data obtained at the 200 mg/s mass flow rate (T is given in [K]). This

curve is also given in Fig. 11. Below 30 kW a steady state was not yet reached.

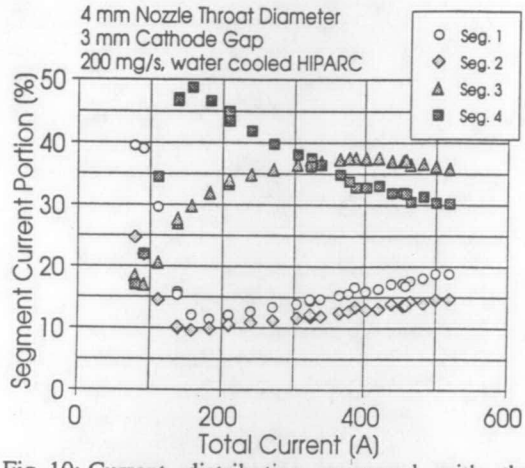

Fig. 10: Current distribution measured with the water cooled HIPARC.

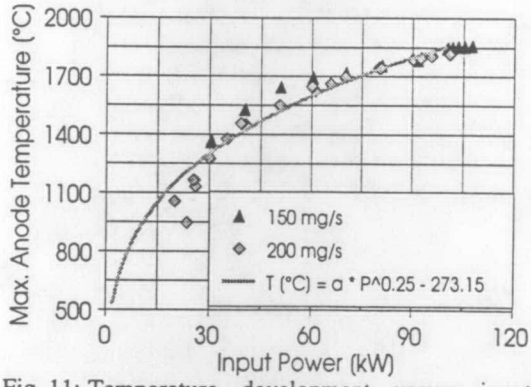

Fig. 11: Temperature development versus input power. Temperatures are measured at a spot on the anode close to the nozzle end.

Electrical Magnitudes

The current/voltage characteristics of HIPARC-R look flatter than the one obtained with the water cooled counterpart; the voltage level is higher (Fig. 12).

The voltage increases with increasing current. This behaviour is typical for MPD devices or arcjet devices at high specific input power. It is to be noted that these data marked with "W" has been obtained with a nozzle throat diameter of 4 mm, where the 100 kW level could be reached only with a mass flow rate of 400 mg/s and where no comparable experiments have been performed yet with HIPARC-R.

Thrust Characterictics

The maximum mass flow rate currently tested with HIPARC-R was 300 mg/s H_2. At a maximum input power of 100 kW a thrust of 4.0 N was measured (Fig. 13). This leads to a specific impulse of almost 1400 s at a specific input power of 338 MW kg^{-1} s^{-1} (Fig. 14). Better performance is reached with lower mass flow rates. At 200 mg/s a specific impulse of almost 1800 s could be achieved at 500 MJ/kg specific input power which equals an absolute input power of 100 kW.

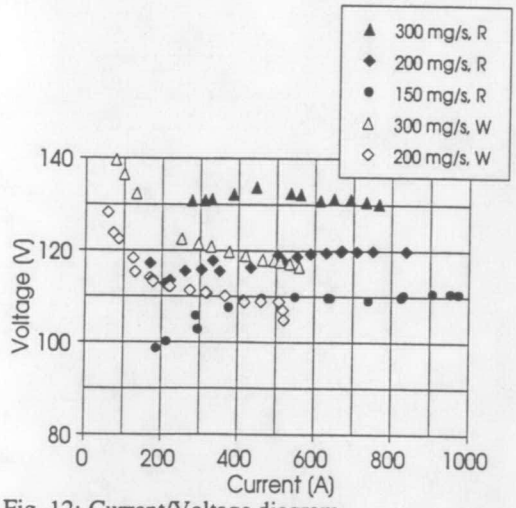

Fig. 12: Current/Voltage diagram
(R: radiation cooled, W: water cooled)

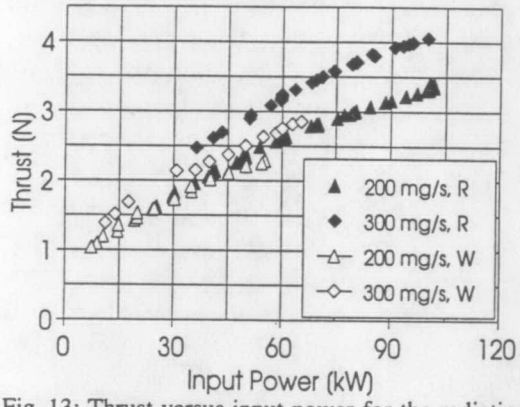

Fig. 13: Thrust versus input power for the radiation cooled (R) and the water cooled (W) thruster.

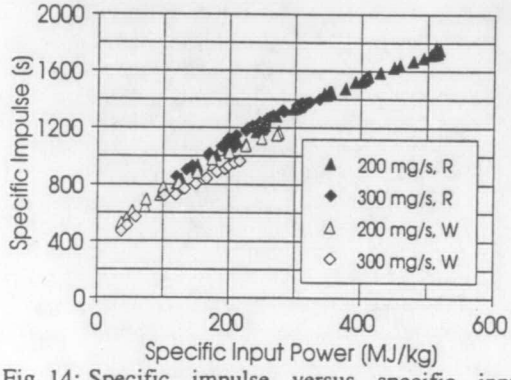

Fig. 14: Specific impulse versus specific input power for the radiation cooled (R) and the water cooled (W) thruster.

The best results in terms of efficiency have been obtained with a mass flow rate of 200 mg/s. The thrust efficiency values range from 25 to 30 %, depending on specific input power (Fig. 15).

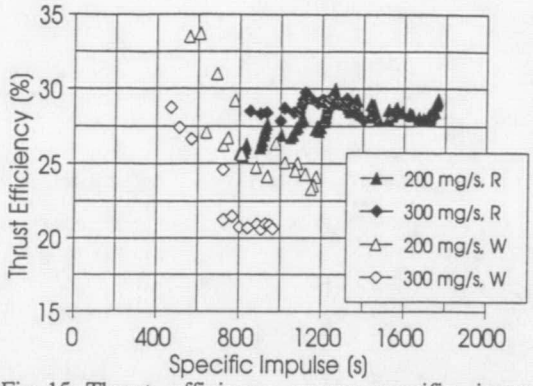

Fig. 15: Thrust efficiency versus specific input power (R: radiation cooled, W: water cooled)

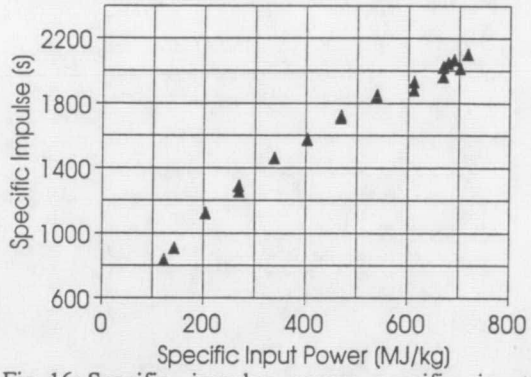

Fig. 16: Specific impulse versus specific input power at 150 mg/s.

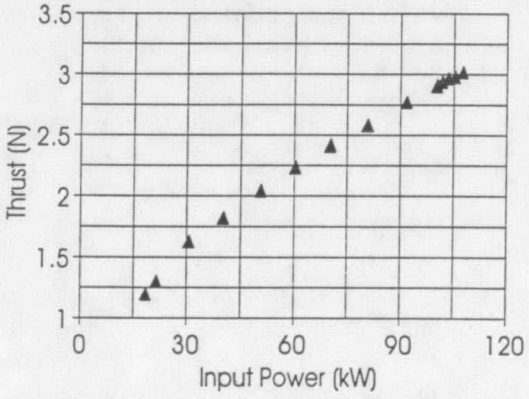

Fig. 17: Thrust versus input power at 150 mg/s.

Encouraged by the thruster performance at high power operation the mass flow rate was throttled down to 150 mg/s in order to increase the specific input power. Here the thruster could be operated in a stable mode as well, with the specific impulse increasing to 2000 s at 700 MJ/kg specific input power. A further increase of the input power was stopped by a failure of the current supply system during an increase of the current. The last current readout was 973 A yielding an input power of 107 kW. The current was limited to 1000 A in this experiment. Fig. 16 shows the specific impulse versus the specific input power for the 150 mg/s mass flow rate. Absolute values are given in Fig. 17, efficiency data is depicted in Fig. 18.

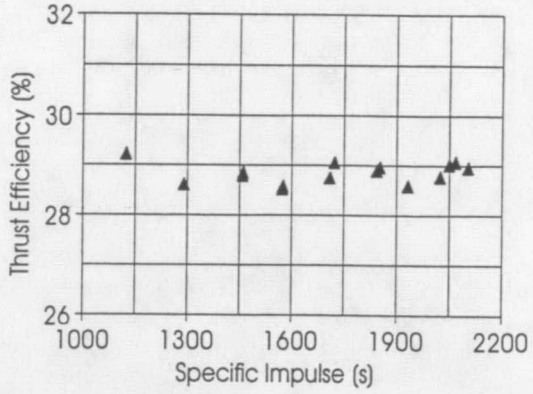

Fig. 18: Thrust efficiency versus specific impulse at 150 mg/s.

In order to determine the portion of thrust that exists because of radiative and regenerative heating effects, the thrust obtained without an arc with a cold thruster was compared with the thrust values at a specified input power value and immediately after switching off this power. This data was compared with equivalent data obtained with the water cooled thruster. Fig. 19 shows this data at different power and mass flow levels. The thrust is divided into three portions:

1. *Cold gas effects:* Thrust originating from cold gas enthalpy transformed to thrust.
2. *Direct arc effects:* Thrust originating from ohmic heating of the propellant gas by the electric arc.
3. *Other heating effects* or *indirect arc effects:* Thrust originating from gas heating by hot thruster structure.

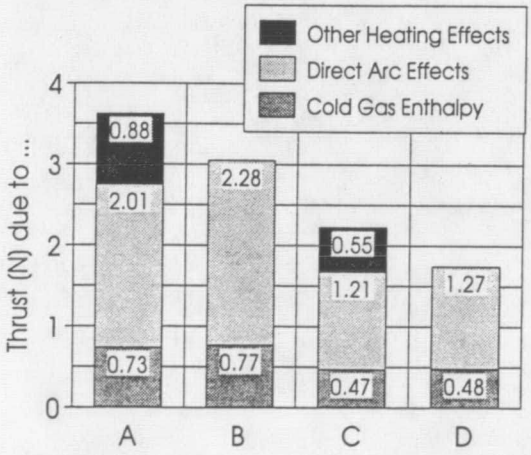

Fig. 19: Thrust portions at different power and mass flow levels. Comparison between HIPARC and HIPARC-R (for nomenclature see next page, Fig. 20).

It can be seen that the cold gas effects and the direct arc effects are significantly larger with the water

cooled thruster type, whereas other heating effects are to be noticed only with the radiation cooled HIPARC-R. The reason for the second observation is clear: The heating effect of the hot cathode tip in a water cooled thruster is very much smaller than the heating effect of the hot structure in a radiation cooled thruster.

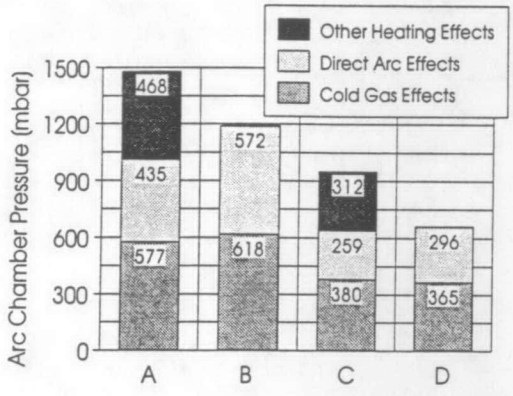

	A	B	C	D
Cooling	Radiation	Water	Radiation	Water
Mass Flow Rate	300 mg/s	300 mg/s	200 mg/s	200 mg/s
Input Power	70 kW	70 kW	35 kW	35 kW

Fig. 20: Distribution of arc chamber pressure portions.

Thrust portions due to direct heating and cold gas effects may be higher with the water cooled device because of two reasons: Firstly, the nozzle throat to exit area ratio is slightly higher with the water cooled device (1:225 cf. 1:258), and secondly the nozzle wall offers slots between the nozzle segments at the water cooled thruster which possibly induce a turbulent boundary layer and prevent the flow from separation.

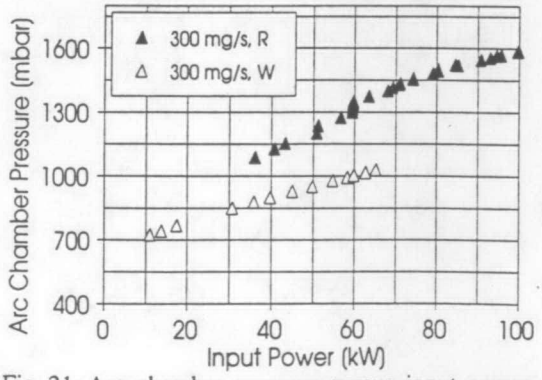

Fig. 21: Arc chamber pressure versus input power at 300 mg/s mass flow rate. Comparison between water cooled (W) and radiation cooled thruster (R).

Arc Chamber Pressure

At a given power setting the arc chamber pressure is higher with the radiation cooled device than with the water cooled thruster (Fig. 20, 21). This indicates a higher average temperature and thus a higher propellant gas enthalpy in the arc chamber.

At the same time the thrust versus arc chamber pressure characteristic shows (almost) straight lines with different slopes for the water cooled and for the radiation cooled thruster version (Fig. 22). The steeper slope yields higher thrust values with the water cooled device at the same value of the arc chamber pressure than with the radiation cooled device. This phenomenon was already discribed in the section before. The equations representing the regression lines are also given in Fig. 22.

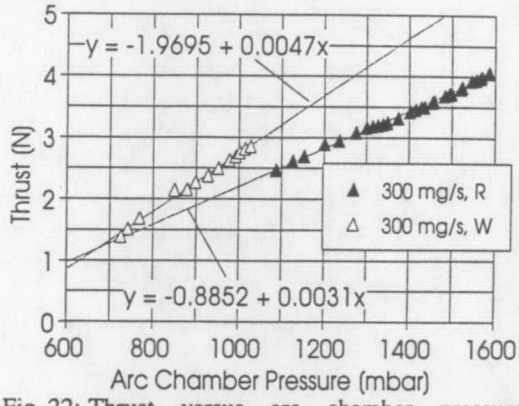

Fig. 22: Thrust versus arc chamber pressure. Comparison between water cooled and radiation cooled thruster.

This equations show clearly that a linear characteristic would lead to negative thrust at low pressure values.

Conclusions

It is shown that a 100 kW thermal arcjet can be operated steady state in a high specific impulse mode. Specific impulse values of more than 2000 s can be realized.

The most critical part in these experiments has been the thermal load on the thruster. The lower the mass flow rate, the less cooling effect can be supported by the propellant gas, even with especially designed regeneratively cooled thrusters. On the other hand, the experiments have shown that high specific impulse operation first of all requires a high specific input power. It is shown that a thermal arcjet thruster can be operated with a specific input power of more than 700 MJ/kg.

Consequently, new high specific impulse thruster designs require methods of thermal baffling or even active thermal control.

Future Plans

Currently a program code for the numerical calculation of thermal arcjet performance is under development. It is mainly based on the MPD calculations already performed at the IRS [9].

In the near future measurements of plasma velocity, and electron densities and electron temperature by means of electrostatic probes will take place. These measurement data will be used for verification of the numerical results.

Acknowledgements

This research was supported partly by the NASA Grant No. NAGW-1736 until 1992, then it was partly supported by the Deutsche Forschungsgemeinschaft (DFG, German Research Society). This support is greatly acknowledged.

The thruster was manufactured by the instruction workshop of the Mercedes-Benz AG, Stuttgart-Untertürkheim, Germany. This support is also greatly acknowleged.

References

[1] T.M. Gölz, M. Auweter-Kurtz, and H.L. Kurtz: *"100 kW Hydrogen Arcjet Thruster Experiments"*, AIAA-92-3638, 28th Joint Propulsion Conference, Nashville, TN, 1992

[2] T.M. Gölz et al.: *"High Power Arcjet Thruster Experiments"*, IEPC-91-072, 22nd IEPC, Viareggio, Italy, 1991

[3] B Glocker, M. Auweter-Kurtz, T.M. Gölz, H.L. Kurtz, H.O. Schrade: *Medium Power Arcjet Thruster Experiments*, AIAA 90-2531, Int. Electric Propulsion Conference, Orlando, Fl., 1990

[4] B. Glocker, M. Auweter-Kurtz: *"Numerical and Experimental Constrictor Analysis of a 10 kW Thermal Arcjet"*, AIAA 92-3835, 28th Joint Propulsion Conference, Nashville, Tenn., July 1992

[5] J.M. Sankovic, F.M. Curran: *"Arcjet Thermal Characteristics"*, AIAA-91-2456, 27th Joint Propulsion Conference, Sacramento, Cal., 1991

[6] H.L. Kurtz, M. Auweter-Kurtz, B. Glocker, W. Merke, H.O. Schrade: *A 15 kW Experimental Arcjet*, IEPC-88-107, 20th International Electric Propulsion Conference, Garmisch-Partenkirchen, FRG, 1988

[7] O.R. Loesener et.al.: *"Linear Pyrometer for Investigations of Thermal Protection Systems"*, Journal of Thermophysics and Heat Transfer, Vol. 7, No. 1, Jan.-March 1993, pp. 82-87

[8] James E. Polk et.al.: *"Mechanisms of Hot Cathode Erosion in Plasma Thrusters"*, AIAA-90-2673, 21st International Electric Propulsion Conference, Orlando, FL, 1990

[9] P.C. Sleziona, M. Auweter-Kurtz, and H.O. Schrade: *"Numerical Calculation of a Nozzle Type and Cylindrical MPD Thrusters"*, AIAA 92-3296, 28th Joint Propulsion Conference, Nashville, Tenn., July 1992